Flow Pattern Transition in a Large Jetting Fluidized Bed with Double Nozzles

Qingjie Guo, Zhi Tang, and Guangxi Yue
Dept. of Thermal Engineering, Tsinghua University, Beijing 100084, P. R. China

Zhenyu Liu and Jiyu Zhang
State Key Laboratory of Coal Conversion, Institute of Coal Chemistry, Chinese Academy of Sciences, Taiyuan 030001, P. R. China

An experimental study was conducted in a 500 mm ID, 8,000 mm high jetting fluidized bed with double vertical nozzles using frame-by-frame analysis of experimental videos. Three different flow patterns (separated jets, flow transition, and jet coalescence), with the two jets always coalesce within the penetration depth, were first observed in the jetting fluidized bed. Radial profiles in the fluidized bed were measured with a PC-4 optical fiber probe. Effects of jet gas velocity and nozzle distance on the radial and axial voidage distribution were studied. The bed hydrodynamic behavior was characterized using a deterministic chaotic theory to analyze effects of jet gas velocity, static bed height, and nozzle distance on the correlation dimension, which increased with increasing jet gas velocity and static bed height.

Introduction

The jet in jetting fluidized beds significantly affects the heat and mass transfer, as well as chemical reactions in the jetting fluidized beds. Previous studies of the flow characteristics of jetting fluidized beds mainly focused on jetting fluidized beds with a single jet and the gas distributor. Davidson et al. (1985) reviewed the flow characteristics in such jetting fluidized beds. Knowltan and Hirsan (1980) identified three penetration depth definitions: the deepest penetration depth of jet bubbles into the bed before losing their momentum L_b, the penetration depth of a series of cavities $L_{\max}$, and the penetration depth of a cavity permanently attached to the nozzle $L_{\min}$. Guo et al. (1996) and Luo et al. (1997) studied the voidage distribution in a jetting fluidized bed employing an optic fiber probe. Yang et al. (1986) used pulse injection of tracer particles to survey particle mixing and examined the macroscopic solid circulation behavior with a force probe. Yang et al. (1984), using measured carbon dioxide trace to determine the gas mixing and gas entertainment, deduced that the radial gas velocity profiles in the jet were similar and could be correlated by Tollmien similarity as in a homogeneous jet. Furthermore, the radial gas profiles for various jet velocities and solid loadings were similar.

Compared with the research for jetting fluidized beds with a single nozzle, there have been few investigations of the flow characteristics with multiple jets in the fluidized bed. Instead, researchers have concentrated their attention on the multiple jets in the gas distributor. Darton et al. (1977) found that coalescence of bubbles in fluidized beds caused the bubble size to increase with distance above the distributor and then suggested a simple equation for the coalescence bubble diameter. Horio and Nonaka (1987) presented a generalized bubble diameter correlation for gas-solid fluidized beds which could be applied for both Geldart group A particles and group B particles. Studies of the grid zone in a shallow fluidized bed (Fakhimi et al., 1983) showed that a stagnant region existed between two adjacent jets. Note that since the free area in the distributor is always less than 3%, the hole pitch is relatively large. The flow characteristics in the distributor area are quite different from those in the jetting fluidized bed.

However, several articles have been recently published about the interaction between gas streams entering the bed from two or more separate nozzles. Recently, Yates et al. (1995) employed the UCL X-ray facility to determine the

Correspondence concerning this article should be addressed to Q. Guo.

bubble coalescence height in a 200×300 mm rectangular cross section fluidized bed with two nozzles, which was correlated by the following equation

$$\frac{h_c}{H_{mf}} = 0.57\left(\frac{1}{d_0}\right)\left(\frac{u_0}{u_{mf}}\right)^{-1/3} \quad (1)$$

Luo et al. (1997) utilized a multipitot tube system to measure the jet momentum in a bed with two nozzles. They found single peak distribution and double peak distributions in the gas momentum distribution in horizontal directions.

There have been few studies of flow pattern transition in large jetting fluidized beds with double vertical nozzles. The objective of this work is to present a comprehensive set of flow pattern transition experiments for the separated jet, the flow transition, and the jet coalescence in a jetting fluidized bed, as well as to develop a correlation for predicting flow pattern transition using dimensional analysis. The voidage distribution in the fluidized bed was also measured simultaneously with an optic probe. Chaotic theory was used to analyze the flow characteristics in the bed, and effects of jet gas velocity and nozzle distance on the correlation dimension were also investigated.

Experimental Apparatus

The experiments were carried out in a semicircular column with 0.5 m ID and 8 m in height. The experimental apparatus is illustrated in Figure 1. Air from three Roots blowers was fed to one nozzle and a semiconical gas distributor. Air to the other nozzle was supplied by a compressor. The air flow rate was measured by four rotometers before injection into the bed. At the bed exit, the solids are separated from the air by a cyclone and return to the fluidized bed. The front plate was made of Plexiglas to allow observation of flow phenomena in the bed. The semiconical gas distributor has a 70° cone angle and was 0.68 m in height. The segregating column had a diameter of 0.27 m and a height of 0.61 m. The two 0.042 m ID semicircular nozzles were vertical 11 mm from the front plate with exits 0.19 m above the top of the semiconical gas distributor. The distance between the two nozzle axes was defined as the nozzle distance. The nozzle distance could be adjusted to vary the experimental conditions. The bed depth was defined as the height from the jet nozzles exit to the dense phase bed surface with the background air at a minimum fluidization and without the jet flow. The bed was operated with depths of around 370 mm, 400 mm, 450 mm, and 660 mm. The back transparent bed window had seven instrumentation ports located at 0.16 m, 0.19 m, 0.25 m, 0.31 m, 0.37 m, 0.43 m, and 0.49 m above the nozzle exit, where measuring probes could be introduced into the bed. Millet (Geldart Group D) with a density of 1,474 kg/m^3 and mean diameter of 1.64 mm was used as fluidized material.

Three pressure probes made of 5 mm ID copper pipe were installed along the bed and connected to pressure transducers (Micros Switch 140PCO1D). These three transducers were located at axial heights of 0.11 m, 0.19 m, and 0.31 m along the back window above the gas distributor. The jet collapse positions were always around 0.31 m above the nozzle exit. Thus, the pressure signal at 0.25 m was suitable for investigating the bed dynamic behavior. The transducer working range was 5,000 Pa. The outside opening of each pressure probe was connected to one of the two input channels of a pressure transducer, which produces an output voltage proportional to the pressure difference between two channels. The remaining channel was exposed to the atmosphere. Solid particles were prevented from entering the pressure probes by a piece of stainless steel screen (200 mesh) soldered to the tip of each pressure probe. All pressure signals were sampled with a sampling system (12 bit, DAS MAX181) at a frequency of 111 Hz for 40 s. For each experimental run, images of the bed were recorded for 180 s using an International M-7 recorder. The images were then analyzed frame by frame with a Panasonic HD-100 player. The frames were also converted to the MPEG format for detailed computer analysis.

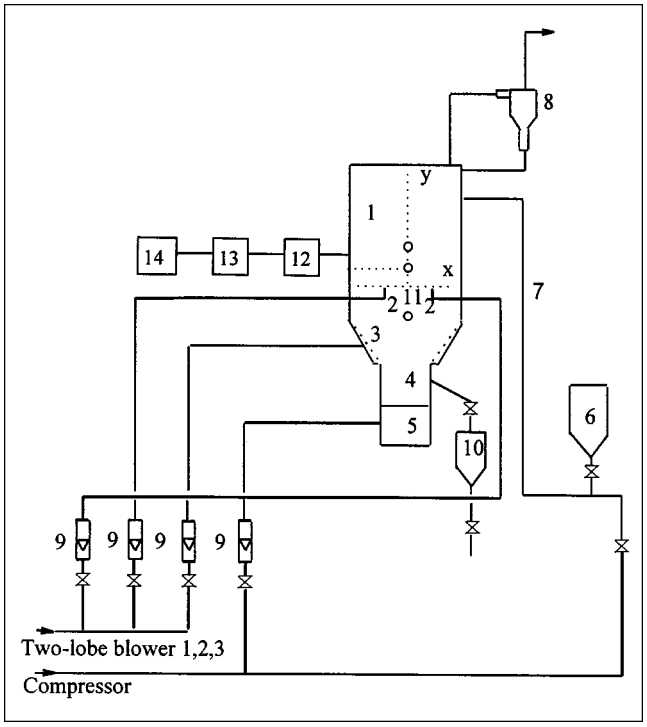

Figure 1. Large jetting fluidized bed with two nozzles.

(1) Jetting fluidized bed; (2) nozzle; (3) semicircular distributor; (4) segregating column; (5) plenum chamber; (6) material tank; (7) conveying pipes; (8) cyclone; (9) rotometer; (10) discharge tank; (11) origin (12) differential pressure sensor; (13) A/D converter; (14) computer.

The particle concentration distributions in this study were measured with a PC-4 optic fiber probe. A detailed description of the probe was given by Zhou et al. (1994) and Guo et al. (2000). Experiments indicated that a sampling time of 30 s was sufficient for the PC-4 probe to obtain repeatable particle concentration curves.

Results and Discussion

Operating pattern

Typical pictures of separated jets for $N_d = 0.28$ m and $u_0 = 32.15$ m/s are shown in Figure 2. The two jets ascend independently within the penetration depth, with bubbles detach-

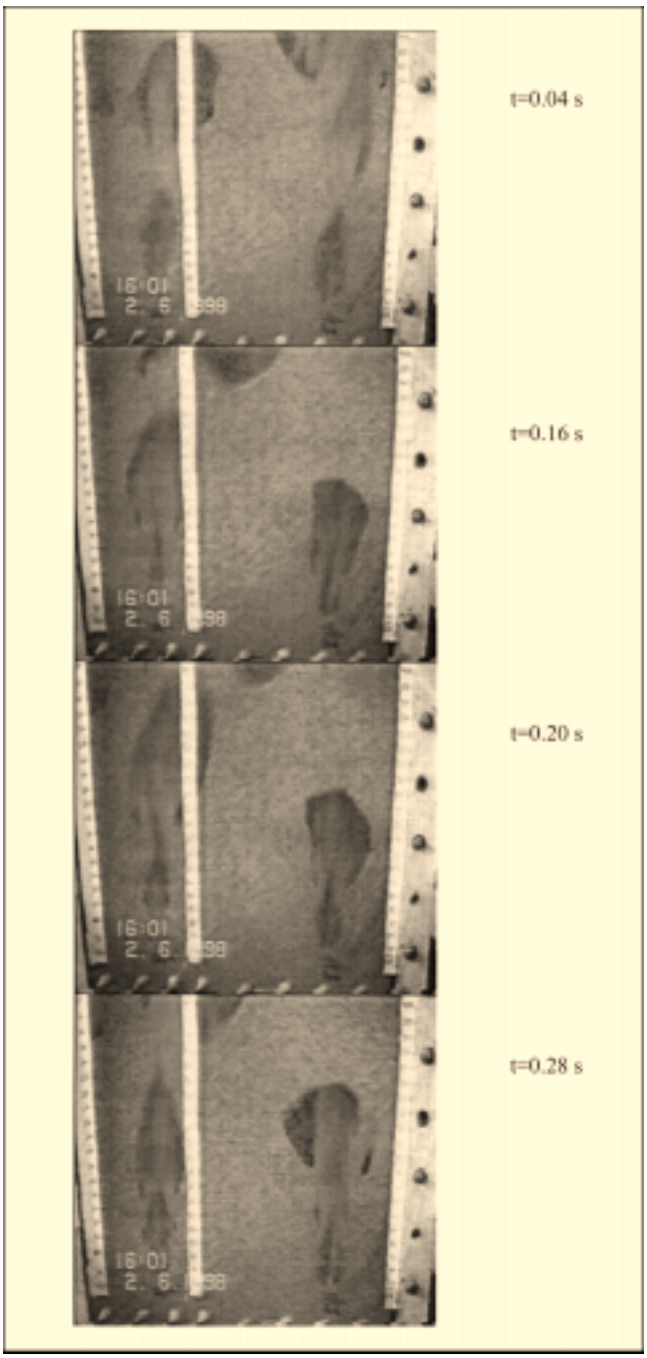

Figure 2. Typical separated jets development (N_d = 0.28 m, u_0 = 32.15 m/s).

ing from the end of the jets, similar to that in a jetting fluidized bed with a single jet. The starting time is defined as the right jet begins to form. Figure 2 shows that the right jet begins to form at $t = 0.04$ s, while the left jet is already well formed. It can be seen from this figure that some particles are entrained into the right jet. Figures 2b and 2c reveal more particles entrained into the right jets and the left jet collapsing. In Figure 2d, the right conical jet continues to increase in size with particles obviously entrained into the right jet, while the left jet has collapsed completely. Note that formation, growth, and collapse of the two jets are asynchronous in most cases, but have the same jet formation frequency. The jet formation frequency, which is the average formation frequency of two jets, increases with increasing jet gas velocity (Figure 3). Generally, the two jets have the same jet formation frequencies when their jet gas velocities are equal. The jet formation frequency in a large jetting fluidized bed with a single nozzle was reported by Ettehadieh et al. (1988) and Guo et al. (1999) to be much smaller than the 5–8 Hz measured by Rowe et al. (1979) and the 20 Hz measured by Hsing and Grace (1978) for small beds due to much larger initial bed heights and jet nozzle sizes in Ettehadieh et al.'s investigations and ours in contrast to Rowe et al.'s and Hsing and Grace's experimental apparatuses. When the nozzle distance was decreased to 0.23 m and the gas jet velocity was increased from 21.4 m/s to 50.9 m/s, two types of flow patterns appeared simultaneously, that is, separated jets (1) with jets independently growing to the penetration depth and jet coalescence (2) with the two jets coalescing into one jet within the jet penetration depth, as shown in Figure 4. The flow transition pattern is defined as the jet coalescence pattern, and the separated jet pattern alternately appears. Figure 5 shows results relating the jet gas velocity to the frequency of jet formation and jet coalescence frequency at $N_d = 0.23$ m. This figure indicates that the flow behavior of the two jets not only depends on the nozzles distance, but also on the jet gas velocity. Since the jets do not coalesce within the jet region for jet gas velocity from 16.07 m/s to 21.43 m/s, the jet formation frequency increases with jet gas velocity. On the other hand, the jet formation frequency decreases for jet gas velocity from 21.43 m/s to 50.9 m/s. In comparison with jet formation frequency, the jet coalescence frequency is increased with increasing jet gas velocity. This can be attributed to two effects. The first is that increasing jet gas velocity and the jet gas momentum increases the jet region, so the probability of jet coalescence increases. The second effect is that the time difference between the two jets starting is large enough so that the two jets grow independently. When the nozzle distance is decreased to 0.18 m, the two jets always coalesce into a single jet near the nozzle exit, as indi-

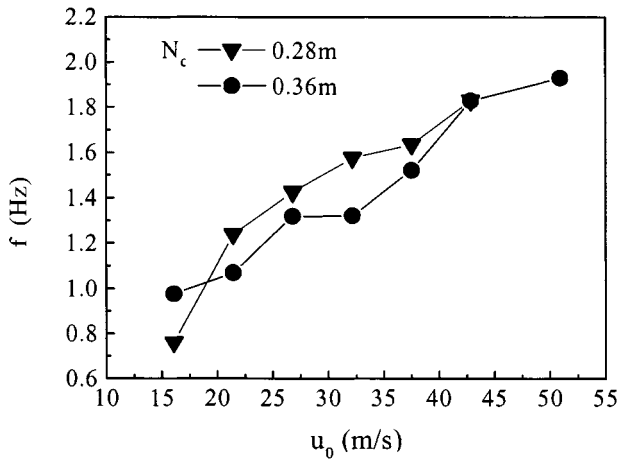

Figure 3. Effect of jet gas velocity on jet formation frequency at N_d = 0.36 m and 0.28 m.

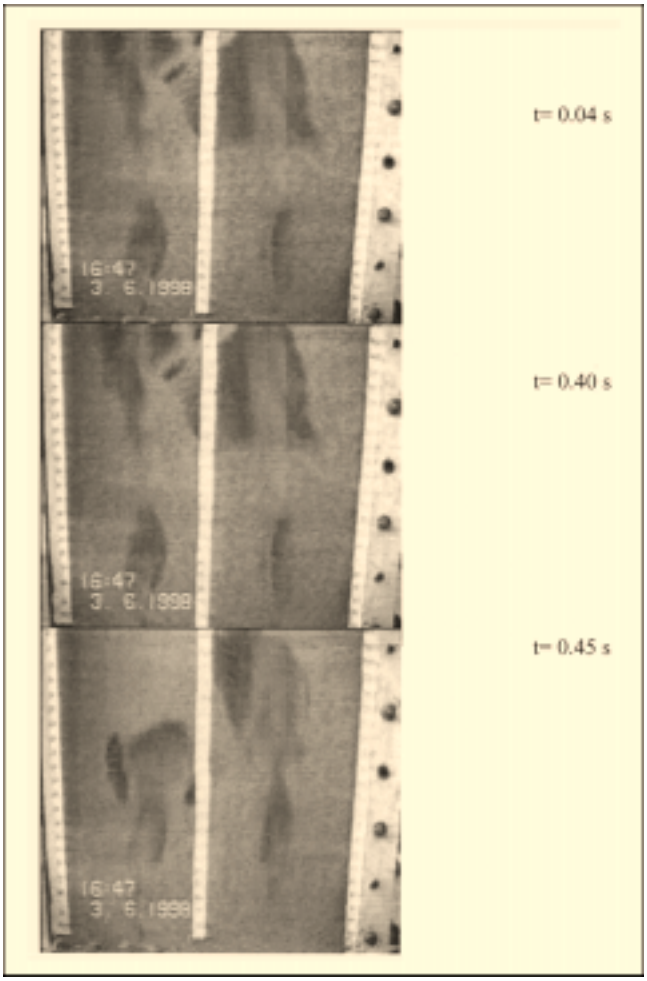

Figure 4. Typical flow transitional pattern.

$N_d = 0.23$ m, $u_0 = 32.15$ m/s.

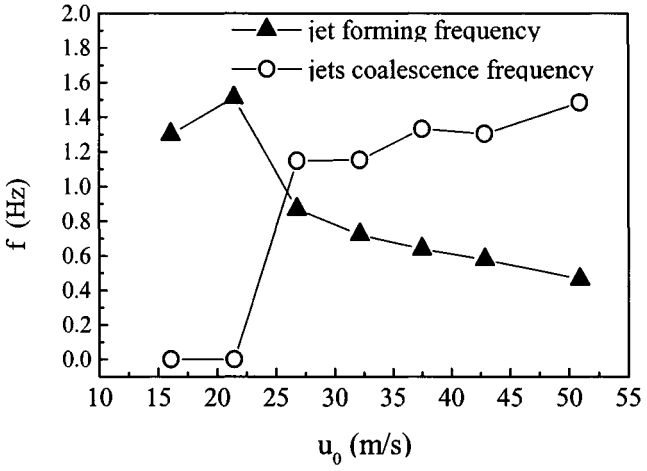

Figure 5. Effect of jet gas velocity on jet formulation and jet coalescence frequency for $N_d = 0.23$ m.

cated in Figure 6 because the two jets entrain each other as the flow around each jet pulls the other jet forward. In this case, the jet coalescence height replaces the penetration depth. Guo et al. (2000) defined the height from nozzle exit to the coalescence point as the jet coalescence height and presented a correlation for the jet coalescence height. Since jet coalescence results in the rapid loss of jet momentum, the jet gas quickly dissipates into the emulsion phase. Hence, the jet coalescence height is often less than the penetration depth. At $N_d = 0.10$ m, the two jets coalesce as soon as they leave the nozzle exit. Figure 7 shows that the frequency of jet coalescence for $N_d = 0.10$ m is slightly less than that for $N_d = 0.18$ m since the smaller nozzle distance brings about more jet momentum loss.

Flow pattern transition map and correlation

As discussed above, the penetration depth is a critical parameter to distinguish the three flow patterns (separated jets, flow transition, and jet coalescence) in the jetting fluidized bed with two vertical nozzles. Previous studies (Yang and Keairns, 1979; Guo et al., 1999) showed that the penetration depth is a function of nozzle diameter, jet gas velocity, gas density, particle density, and gravitational acceleration. In this jetting fluidized bed with double nozzles, Guo et al. (2000) also found that the penetration depth decreases with decreasing nozzle distance at the same jet gas velocity. Therefore, the penetration depth is a function of six variables

$$L_j = f(d_0, u_0, \rho_g, \rho_p, g, p) \tag{2}$$

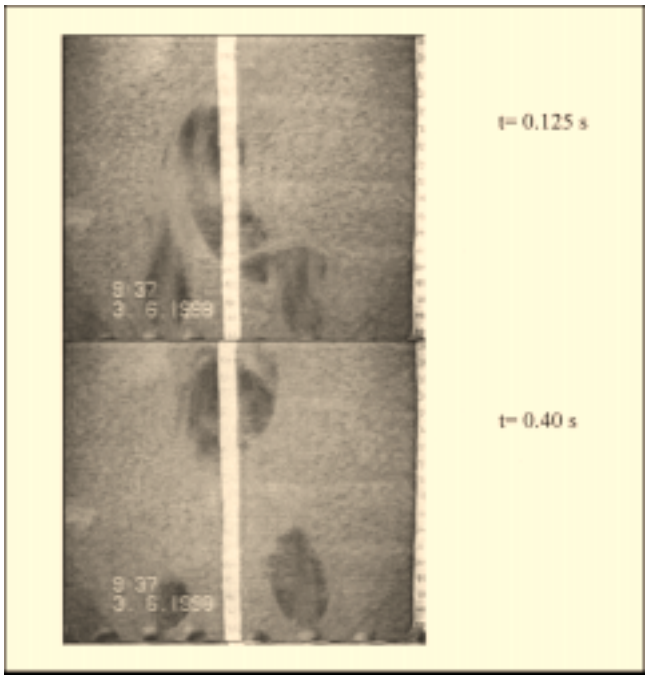

Figure 6. Typical jet coalescence pattern ($N_d = 18$ m, $u_0 = 21.43$ m/s).

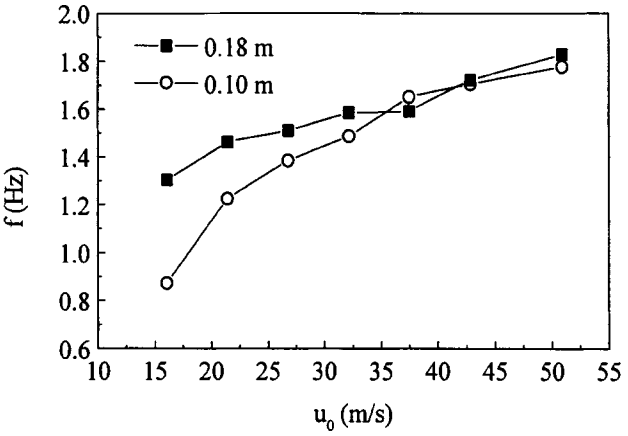

Figure 7. Jet coalescence frequencies for small nozzle distance.

Because there are three basic dimension (length, mass, and time) in Eq 2, this equation may be rewritten in the following dimensionless form

$$\frac{L_j}{d_0} = F\left(\frac{\rho_g u_0^2}{\rho_p g d_0}, \quad \frac{p}{d_0}\right) = \left(F_r^*, \frac{p}{d_0}\right) \tag{3}$$

$$F_r^* = \frac{\rho_g}{\rho_p - \rho_g}\frac{u_0^2}{g d_0}$$

Generally speaking, the separated jet pattern, which appears with greater nozzle distance, is defined as jets existing independently within the jet penetration depth. As the nozzle distance decreases, the two jets either coalesce or continue to grow independently within the penetration depth. As the nozzle distance is decreased further, the two jets always coalesce within the jet region, even for low jet gas velocity. Coalescence within the penetration depth is defined as the jet coalescence pattern. Frame-by-frame analysis of the various jet gas velocities at different nozzle distances was used to draw the flow pattern map in Figure 8. The boundary between the jet coalescence pattern and the flow transition pattern is

$$F_r^* = 14.2\left(\frac{p}{d_0} - 4.12\right) \tag{4}$$

The boundary between the flow transition pattern and the separated jet pattern is expressed as

$$\frac{p}{d_0} = 6.2 \tag{5}$$

Pressure Fluctuation in Jetting Fluidized Beds

$$\bar{p} = \frac{1}{n}\sum_{i=1}^{n} p_i \tag{6}$$

$$\sigma = \sqrt{\frac{1}{n-1}\sum_{i=1}^{n}(p_i - \bar{p})^2} \tag{7}$$

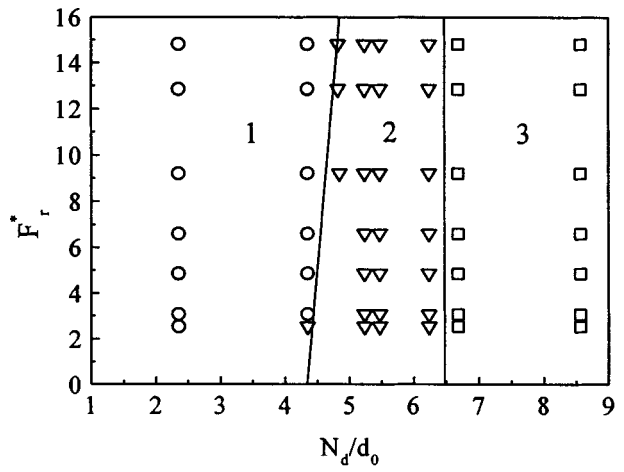

Figure 8. Flow pattern.

(1) Jet coalescence pattern; (2) flow transition pattern; (3) separated jet pattern.

The influence of jet gas velocity on the mean pressure fluctuation at five nozzle distance is shown in Figure 9. For N_d = 0.36 m, the mean pressure fluctuation has small variations since two jets are in the separated jet pattern. As the nozzle distance decreases (N_d = 0.23 m), the mean pressure fluctuation fluctuates strongly as the jets coalesce at the bed axis. The bed height expanded with large fluctuations with increasing jet gas velocity. Furthermore, the jets coalescence frequency increases with decreasing nozzle distance. When N_d was further decreased to 0.18 m or 0.10 m, the mean pressure fluctuation increases more with jet gas velocity since the two jets always coalesced.

Effect of jet gas velocity on the correlation dimension

The correlation dimension used in the deterministic chaos theory denotes the degree of freedom in the attainable states of the system (degree of complexity), which is determined from the slope of the linear part of a log-log plot of the

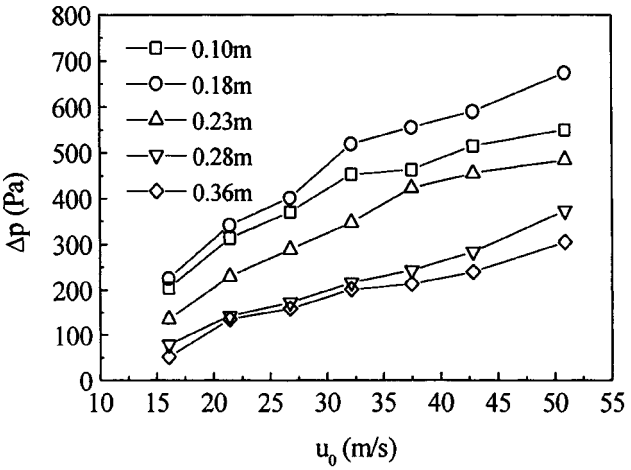

Figure 9. Mean pressure fluctuations for various nozzle distances.

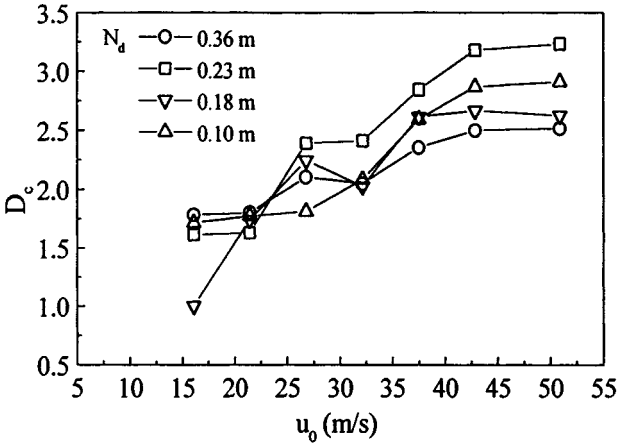

Figure 10. Effect of jet gas velocity on the correlation dimension for different nozzle distance.

$H_0 = 0.66$ m.

Grassberger-Procaccia (1983) correlation integral vs. the radius of a given hyper sphere in the phase space. The influence of the jet gas velocity on the correlation dimension for different nozzle distances is shown in Figure 10. The correlation dimension tends to increase with increasing jet gas velocity. For the 0.36 m nozzle distance, the large jet gas velocity results in a large penetration depth; thus, the bubble diameter is large and the probability of jet and bubble coalescence increases. When the nozzle distance is equal to 0.18 m or 0.10 m, and the two jets always coalesce and grow as a single jet in the fluidized bed, the trend of the correlation dimension variation indicates that the jet coalescence frequency increases with increasing jet gas velocity. Note that for N_d equal to 0.23 m, the curve of the correlation dimension vs. jet gas velocity reaches a maximum increasing rate because the flow structure is the most complex with separated jets and with jets and bubbles coalescing in the jet region.

Figure 11 illustrates the effect of the bed height on the correlation dimension. The correlation dimension increases

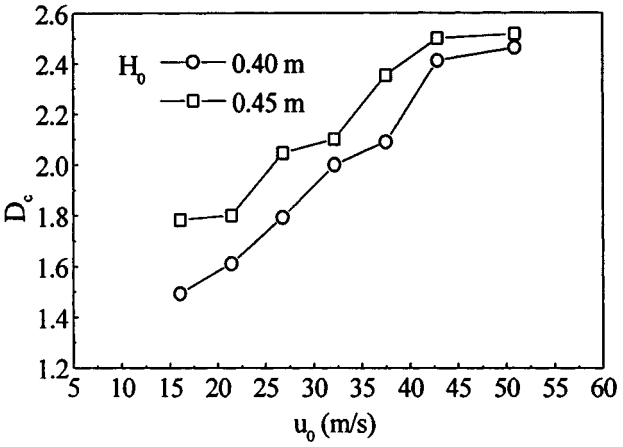

Figure 11. Effect of jet gas velocity on the correlation dimension for different static bed heights.

$N_d = 0.36$ m.

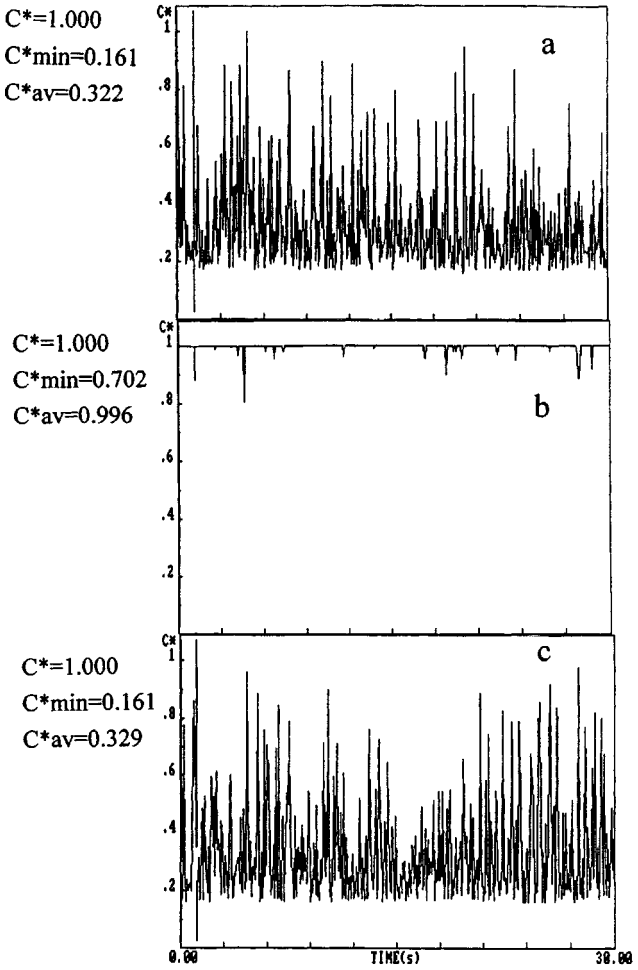

Figure 12. (a, c) Typical particle concentration fluctuations in the jet region; (b) the emulsion phase.

$N_d = 0.36$ m, $H_0 = 0.66$ m, $u_0 = 42.9$ m/s. (a) −0.216 m, 0.16 m; (b) 0 m, 0.16 m; (c) 0.216 m, 0.16 m.

with increasing static bed height, which differs from the conclusions obtained by other researchers. Hay et al. (1995) stated that the static bed height had little effect on the correlation dimension, while van den Bleck et al. (1993) reported that the static bed height had some effect on the correlation dimension. Further investigations are needed to clarify this relationship.

Radial voidage distribution

A typical particle concentration variation is shown in Figure 12 for N_d of 0.36 m and u_0 of 45.3 m/s. The curves in Figure 12, which represent observation over a 30-s time span, show significant oscillations in the local instantaneous solid concentration. The PC-4 optic probe analysis program calculated time-averaged solid concentration to be 0.322 at 0.16 m above the nozzle exit, as shown in Figure 12a. The data in Figures 12a and 12c with symmetry abscissa show that the particle concentration in the jet region which has the almost same value fluctuates strongly with many peaks. Each peak

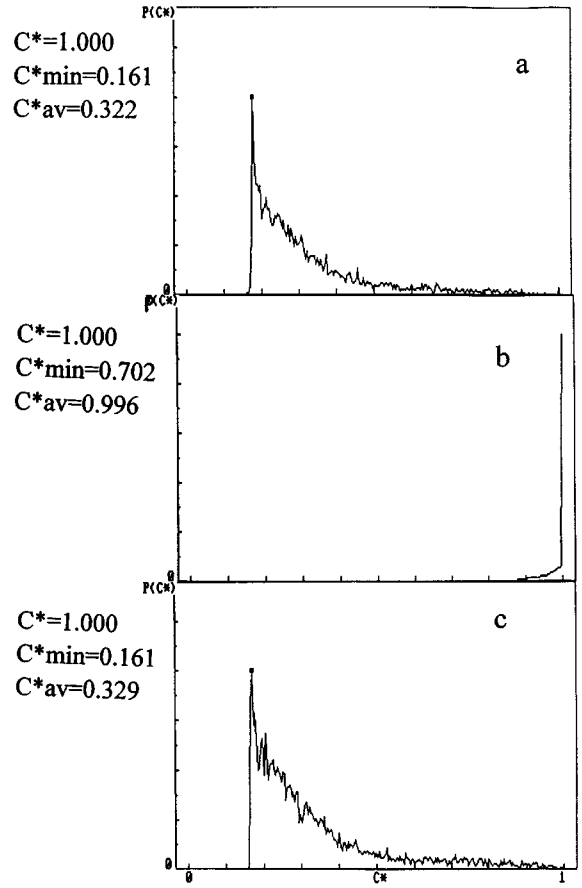

Figure 13. (a, c) Typical probability distributions of particle concentrations in the jet region; (b) emulsion phase.

$N_d = 0.36$ m, $H_0 = 0.66$ m, $u_0 = 42.9$ m/s. (a) -0.216 m, 0.16 m; (b) 0 m, 0.16 m; (c) 0.216 m, 0.16 m.

represents a jet crossing the tip of the probe, so the jet formation frequency can be represented by counting the number of peaks. The result agreed well with the results of the frame-by-frame video analysis. The variation of the particle concentration curve with minor fluctuations in the emulsion region (Figure 12b) can be attributed to gas diffusion from the jet region to the emulsion region. Typical probability distributions of the particle concentrations in the two jets regions and the emulsion phase region are presented in Figure 13. Figures 13a and 13c have one peak with a wide distribution indicating particles are continuously entrained into the jet region. An almost linear distribution appears in Figure 13b, representing small particle concentration fluctuations in the emulsion phase region.

The mean voidage as a function of radial position at large nozzle distance is plotted vs. axial position in Figure 14a. Each radial voidage profile can be divided into two parts: the jet region and the emulsion region between the two jet regions. The voidage profile is elliptic in the jet region and almost flat in the emulsion region. The voidage distribution in the jet region was also described as elliptic by Guo et al. (1996) and Luo et al. (1997). Note that the voidage in the emulsion region is equal to that in the minimum fluidization condition.

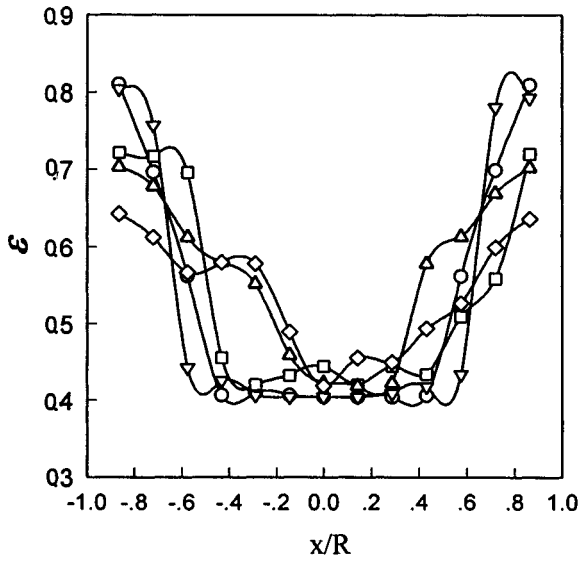

Figure 14a. Radial voidage distribution in the jetting fluidized bed.

$N_d = 0.36$ m, $H_0 = 0.66$ m, $u_0 = 42.8$ m/s. y ○ 0.16 m; ▽ 0.19 m; □ 0.31 m; △ 0.37 m; ◇ 0.49 m.

With increasing height, the range of the elliptic distribution expands since the jet continuously entrains particles and the jet region expands. Also, the two elliptic profiles at a height of 0.49 m show that the two jets rise independently. The effect of nozzle distance on the radial voidage distribution is observed by comparing Figure 14b and Figure 14a. At $y = 0.16$ m, the radial voidage distribution includes three portions: part one is the two jet regions; part two is the two emulsion regions near the bed wall; and part 3 is the high concentration region between the two jets. Only one elliptic profile appears at $y = 0.19$ m due to the coalescence of the two jets.

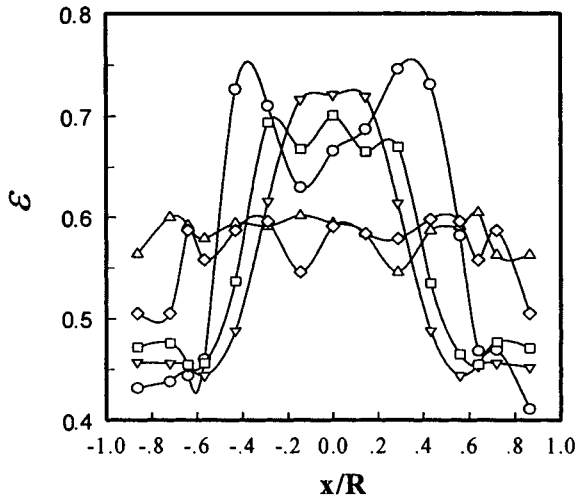

Figure 14b. Effect of nozzle distance on the radial voidage distribution in the jetting fluidized bed.

$N_d = 0.18$ m, $H_0 = 0.66$ m, $u_0 = 42.9$ m/s. y ○ 0.16 m; ▽ 0.19 m; □ 0.31 m; △ 0.37 m; ◇ 0.43 m.

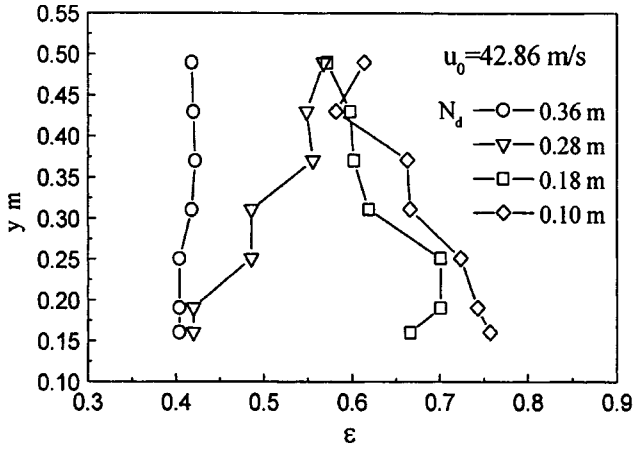

Figure 15. Axial voidage profiles for various nozzle distances.

The time-averaged voidage distributions along the axial direction are presented for a variety of nozzle distances in Figure 15. The voidage at various axial locations is equal to that at the minimum fluidization condition when the nozzle distance is 0.36 m, because the axial positions for $N_d = 0.36$ m are always in the emulsion region, which is consistent with Figure 15a. For the nozzle distance of 0.28 m, the voidage distributions at both 0.16 m and 0.19 m from the nozzle exit indicate that these two axial positions are still in the emulsion region. However, the voidage at axial position of 0.25 m has a large increase due to the fact that the two jets have entrained gas and solids and have widened. It should be pointed out that jet coalescence does not take place at $y =$ 0.37 m. For small nozzle distances ($N_d = 0.18$ m and 0.10 m), the two jets coalescing at an axial height of 0.19 m results in the larger voidage. The axial voidage profile has a ''s'' distribution, which further supports the observation that the two jets coalesce into a single jet near the nozzles and then rises as one jet, as shown in Figure 6.

Conclusions

The frame-by-frame analysis of experimental video indicated the existence of three flow patterns, that is, the separated jet, the flow transition, and the jet coalescence occurring in turn with decreasing nozzle distance for the range of jet gas velocities in this study. The experimental data were used to draw a flow transition map and develop the equations for the flow transitions.

The relationship between the mean pressure fluctuations and various nozzle distances shows that the decreasing nozzle distance results in greater pressure variation.

Deterministic chaos theory was used to investigate the flow characteristics in the jetting fluidized bed. The correlation dimension increases with increasing jet gas velocity for a given static bed height. The maximum increasing rate the correlation dimension vs. jet gas velocity for $N_d = 0.23$ m shows that this flow structure is the most complex. Higher static bed height leads to high correlation dimension.

For larger nozzle distances and lower axial heights, the radial voidage distribution is divided into two parts: part 1 is the jet region where the voidage profile is elliptic while part 2 is the emulsion phase where the voidage equals that of the minimum fluidization condition. At larger axial heights, the parabolic profiles show that the two jets can exist independently.

For smaller nozzle distance, the radial voidage distribution at low axial positions (flow transition pattern and jet coalescence pattern) consists of three parts: the jet region, the high concentration region and the emulsion region between the jet region and the bed wall. The radial voidage at greater heights for the smaller nozzle distance is only a single parabolic which suggests that the two jets have coalesced into one jet within the jet region.

The axial profile in the separated jet pattern varies little. However, axial voidage profile in the coalescence pattern has an ''s'' profile which illustrates that the two jets coalesce into one jet.

Notation

C^* = instantaneously particle fluctuation
$C^*\max$ = maximum particle concentration
$C^*\min$ = minimum particle concentration
$C^*\text{av}$ = average particle concentration
d = nozzle diameter, m
Dc = correlation dimension
F_r^* = two-phase Froude number
g = gravitational acceleration, m/s^2
h_c = bubble coalescence height, m
H_{mf} = settled bed height at minimum fluidization condition, m
H_0 = static bed height, m
l = nozzle distance in Eq. 1
L_j = penetration depth, m
L_b = deepest penetration depth, m
$L_{\max}$ = maximum penetration depth, m
$L_{\min}$ = minimum penetration depth, m
n = sampling point number
N_d = nozzle distance between two nozzles, m
p_i = instantaneous pressure at various time, Pa
$P(C^*)$ = probablity distribution of particle concentration
$\bar{p}$ = average pressure, Pa
u_{mf} = minimum fluidization velocity, m/s
u = gas jet velocity, m/s
x = abscissa, m
y = ordinate, m
ϵ = voidage
ρ_g = fluidization gas density, kg/m^3
ρ_p = particle density, kg/m^3
σ = mean pressure fluctuation, Pa

Literature Cited

Davidson, J. F., R. Clift, and D. Harrison, *Fluidization,* 2nd ed., Academic Press, London (1985).

Darton, B. C., R. D. Lanauze, J. F. Davison, and D. Harrison, ''Bubble Growth Due to Coalescence in Fluidized Beds,'' *Trans. Inst. Chem. Eng.*, **55**, 274 (1977).

Ettehadieh, B., W. Ch. Yang, and G. B. Haldipur, ''Motion of Solids, Jetting and Bubbling Dynamics in a Large Jetting Fluidized Bed,'' *Powder Technol.*, **54**, 243 (1988).

Fakhimi, S., S. Sohrabi, and D. Harrison, ''Entrance Effects at a Multi-orifice Distributor in Gas-Fluidized Beds,'' *Can. J. Chem. Eng.*, **61**, 364 (1983).

Guo, Q. J., J. Y. Zhang, and G. H. Luo, ''Porosity Distribution in Two-dimensional Jetting Fluidized Bed with a Nozzle,'' *Chem. Ind. and Eng.*, **13**(4), 14 (1996).

Guo, Q. J., J. Y. Zhang, and Zh. Y. Liu, ''Chaotic Study on a Large Jetting Fluidized Bed with Two Nozzles,'' *Chem. Reaction Eng. and Technol.*, **15**, 58 (1999).

Guo, Q. J., Zh. Y. Liu, and J. Y. Zhang, ''Flow Characteristics in a Large Jetting Fluidized Bed with Two Nozzles,'' *Ind. Eng. Chem. Res.*, **39**, 746 (2000).
Guo, Q. J., ''Study on Flow Characteristics in the Multi-jet Jetting Fluidized Bed,'' PhD Thesis, Inst. of Coal Chemistry, Chinese Academy of Sciences, Taiyuan, P. R. China (1999).
Guo, Q. J., J. Y. Zhang, Zh. Y. Liu, and G. X. Yue, ''Chaotic Study on a Large Jetting Fluidized Bed with a Vertical Nozzle,'' *Chinese J. of Chem. Eng.*, **8**, 176 (2000).
Grassberger, P., and I. Procaccia, ''Estimation of the Kolmogorgov Entropy from a Chaotic Signals,'' *Physica, 9D*, 189 (1983).
Hsing, T. P., and J. R. Grace, *Fluidization*, J. F. Davidsion and K. L. Keairns, eds., Cambridge University Press, Cambridge, U.K., p. 19 (1978).
Hay, J. M., B. H. Nelson, C. L. Briens, and M. A. Bergougnou, ''The Calculation of the Characteristics of a Chaotic Attractor in a Gas-Solid Fluidized Bed,'' *Chem. Eng. Sci.*, **50**, 373 (1995).
Horio, M., and A. Nonaka, ''A Generalized Bubble Diameter Correlation for Gas-Solid Fluidized Beds,'' *AIChE J.*, **33**, 1865 (1987).
Knowlton, T. M., and I. Hirsan, ''The Effect of Pressure on Jet Penetration Depth in Semi-Cylindrical Gas-Fluidized Beds,'' *Fluidization III*, Henniker, NH, Plenum, New York, 315 (1980).
Luo, Ch. H., S. Uemiya, and T. Kojima, ''Dynamic Behavior and Solid Volume Fraction Distribution in a Jetting Fluidized Bed,'' *J. Chem. Eng. Japan*, **30**, 491 (1997).
Luo, G. H., J. Y. Zhang, and B. J. Zhang, ''The Behavior of Gas Flow Ejected from Two Vertical Nozzles in a Fluidized Bed,'' *Chinese J. of Chem. Eng.*, **5**, 280 (1997).
Rowe, P. N., H. J. Macgillivray, and D. J. Cheesman, ''Gas Discharge from an Orifice into a Gas Fluidized Bed,'' *Trans. Inst. Chem. Eng.*, **57**, 194 (1979).
van den Bleek, Cor M., and J. C. Schouten, ''Deterministic Chaos: A New Tool in Fluidized Bed Design and Operation,'' *Chem. Eng. J.*, **53**, 75 (1993).
Yang, W. Ch., ''Comparison of Jetting Phenomena in 30-cm and 3-m Diameter Semicircular Fluidized Beds,'' *Powder Technol.*, **100**, 147 (1998).
Yang, W. C., D. L. Keairns, and D. K. Mclain, ''Gas Mixing in a Jetting Fluidized Bed,'' *AIChE Symp. Ser.*, **80** (234), 32 (1984).
Yang, W. C., B. Ettehadieh, and G. B. Haldipur, ''Solid Circulation Pattern and Particles Mixing in a Large Jetting Fluidized Bed,'' *AIChE J.*, **32**, 1994 (1986).
Yang, W. C., and D. L. Keairns, ''Estimating the Jet Penetration Depth of Multiple Vertical Grid Jets,'' *Ind. Eng. Chem. Fundam.*, **18**, 317 (1979).
Yates, J. G., K. T. Wu, and D. J. Cheesman, ''Bubble Coalescence from the Multiple Entry Nozzles,'' *Fluidization VIII* (Preprints), Tours, France, p. 335 (1995).
Zhou, J., J. R. Grace, S. Qin, C. M. H. Brereton, C. J. Lim, and J. Zhu, ''Voidage Profiles in a Circulating Fluidized Bed of Square Cross-Section,'' *Chem. Eng. Sci.*, **49**, 3217 (1994).

Manuscript received Jun. 8, 2000, and revision received Oct. 25, 2000.